

The bright optical afterglow of the long GRB 001007 ^{★,★★,★★★,†,‡}

J.M. Castro Cerón¹, A.J. Castro-Tirado², J. Gorosabel^{2,3,4}, J. Hjorth⁵, J.U. Fynbo⁶, B.L. Jensen⁵, H. Pedersen⁵, M.I. Andersen⁷, M. López-Corredoira⁸, O. Suárez^{9,4}, Y. Grosdidier⁸, J. Casares⁸, B. Milvang-Jensen¹⁰, G. Mallén-Ornelas¹¹, A. Fruchter¹², J. Greiner¹³, E. Pian¹⁴, P.M. Vreeswijk¹⁵, S.D. Barthelmy¹⁶, T. Cline¹⁶, F. Frontera¹⁷, L. Kaper¹⁵, S. Klose¹⁸, C. Kouveliotou¹⁹, D.H. Hartmann²⁰, K. Hurley²¹, N. Masetti¹⁷, E. Mazets²², E. Palazzi¹⁷, H.S. Park²³, E. Rol¹⁵, I. Salamanca¹⁵, N. Tanvir²⁴, J.I. Trombka¹⁶, R.A.M.J. Wijers²⁵, G.G. Williams²⁶, and E. van den Heuvel¹⁵

¹ Real Instituto y Observatorio de la Armada, Sección de Astronomía, 11.110 San Fernando-Naval (Cádiz) Spain.

² Instituto de Astrofísica de Andalucía (CSIC), Apartado de Correos, 3.004, 18.080 Granada Spain.

³ Danish Space Research Institute, Juliane Maries Vej 30, 2100 Copenhagen Ø Denmark.

⁴ Laboratorio de Astrofísica Espacial y Física Fundamental (INTA), Apartado de Correos, 50.727, 28.080 Madrid Spain.

⁵ Astronomical Observatory, University of Copenhagen, Juliane Maries Vej 30, 2100 Copenhagen Ø Denmark.

⁶ European Southern Observatory, Karl Schwarzschild Straße 2, 85748 Garching Germany.

⁷ Division of Astronomy, PO Box 3000, 90014 University of Oulu Finland.

⁸ Instituto de Astrofísica de Canarias, 38.200 La Laguna (Tenerife) Spain.

⁹ Departamento de Ciencias de la Navegación y de la Tierra, Universidad de la Coruña, 15.011 La Coruña Spain.

¹⁰ School of Physics and Astronomy, University of Nottingham, University Park NG7 2RD Nottingham UK.

¹¹ Department of Astronomy, University of Toronto, 60 St. George Street, Toronto ON M5S 3H8 Canada.

¹² Space Telescope Science Institute, 3700 San Martin Drive, Baltimore MD 21218 USA.

¹³ Astrophysikalisches Institut, An der Sternwarte 16, 14482 Potsdam Germany.

¹⁴ Osservatorio Astronomico di Trieste, Via Tiepolo 11, 34131 Trieste Italy.

¹⁵ University of Amsterdam, Kruislaan 403, 1098 SJ Amsterdam The Netherlands.

¹⁶ Goddard Space Flight Centre (NASA), Greenbelt MD 20771 USA.

¹⁷ Istituto Tecnologie e Studio Radiazioni Extraterrestri (CNR), Via Gobetti 101, 40129 Bologna, Italy.

¹⁸ Thüringer Landessternwarte Tautenburg, 07778 Tautenburg Germany.

¹⁹ Marshall Space Flight Centre (NASA), SD-50, Huntsville AL 35812 USA.

²⁰ Clemson University, Clemson SC 29634 USA.

²¹ University of California, Berkeley, Space Sciences Laboratory, Berkeley CA 94720-7450 USA.

²² Ioffe Physico-Technical Institute, 26 Polytekhnicheskaya, St. Petersburg 194021 Russia.

²³ Lawrence Livermore National Laboratory, Livermore CA 94550 USA.

²⁴ Department of Physical Sciences, University of Hertfordshire, College Lane, Hatfield, Herts AL10 9AB UK.

²⁵ Department of Physics and Astronomy, State University of New York, Stony Brook NY 11794-3800 USA.

²⁶ Steward Observatory, Tucson AZ 85721 USA.

Received / Accepted

Abstract. We present optical follow up observations of the long GRB 001007 between 6.14 hours and ~ 468 days after the event. An unusually bright optical afterglow (OA) was seen to decline following a steep achromatic power law decay with index $\alpha = -2.05 \pm 0.11$, possibly indicating a break in the lightcurve at $t - t_0 < 3.5$ days, as found in other bursts. Upper limits imposed by the LOTIS alerting system 6.14 hours after the gamma-ray event also suggests the presence of a knee in the optical lightcurve. The spectral index β of the OA yields -1.24 ± 0.57 . These values may be explained both by several fireball jet models and by the cannonball model. Fireball spherical expansion models are not favoured. Late epoch deep imaging revealed the presence of a complex host galaxy system, composed at least by two objects located $1.2''$ (1.7σ) and $1.9''$ (2.7σ) from the afterglow position.

Key words. gamma rays: bursts – techniques: photometric – cosmology: observations

Send offprint requests to: J.M. Castro Cerón,
e-mail: josemari@alumni.nd.edu

* Based in part on observations made with the Instituto de Astrofísica de Canarias's 0.82 m telescope, at the Observatorio del Teide, in the island of Tenerife, Spain.

** Based in part on observations made with Denmark's 1.54 m telescope, at the European Southern Observatory, in La Silla, Chile.

*** Based in part on observations made with the Nordic Optical Telescope, operated on the island of La Palma jointly by Denmark,

1. Introduction

Gamma Ray Bursts (GRBs hereafter) are flashes of high energy (~ 1 keV–10 GeV) photons (Fishman & Meegan 1995), occurring at cosmological distances. Observations of GRBs are well described by the so called fireball model in which an explosive flow of relativistic ejecta is released from a central unknown source. Shortly thereafter, the fast moving ejecta sweeps the interstellar matter. The shocked gas powers long lived, broad band emission: the afterglow. This is primarily synchrotron radiation. According to the current view, a forward external shock wave would have produced the afterglow as observed at all wavelengths. Nonetheless, ~ 3000 GRBs have been detected in γ rays and only ~ 25 have been pinpointed at optical wavelengths, with redshifts ranging from $z = 0.0085$ (Galama et al. 1998) to $z = 4.50$ (Andersen et al. 2000). The population of electrons is assumed to be a power law distribution of Lorentz factors Γ_e , following $dN/d\Gamma_e \propto \Gamma_e^{-p}$ above a minimum Lorentz factor $\Gamma_m \geq \Gamma_e$, corresponding to the synchrotron frequency ν_m . The electron distribution power law index is given by p , ranging from 2 to 2.5 for afterglows observed to date (van Paradijs et al. 2000). The electrons radiate synchrotron emission with a flux $F_\nu \propto (t - t_0)^\alpha \nu^\beta$, where α is the temporal decay index, β is the spectral index and $(t - t_0)$ represents the time elapsed since the GRB onset.

The GRB 001007 was detected on 7.207488 UT October 2000 (t_0 hereafter) by the Interplanetary Network (IPN), composed by the Ulysses, Konus-Wind and NEAR spacecraft (Hurley et al. 2000). It exhibited a duration of ~ 375 s, a fluence (25–100 keV) of $\sim 3.3 \times 10^{-5}$ erg cm $^{-2}$ and a peak flux over 0.5 s of 7.1×10^{-7} erg cm $^{-2}$ s $^{-1}$, which places it amongst the brightest GRBs of all kinds. The time history of the GRB as seen by Ulysses and NEAR is presented in Fig. 1. An optical afterglow (OA) was first detected by Price et al. (2000a), then confirmed with further observations, in optical wavelengths, by Castro-Tirado et al. 2000 and Price et al. (2000b) and, in radio wavelengths, by Frail & Berger (2000). Section 2 describes the optical follow up imaging of the GRB 001007 IPN error box. In Sect. 3 we show the characteristics of the OA and its potential host galaxy. The final conclusions are listed in Sect. 4.

2. Observations

Prompt follow up observations started at $t_0 + 6.14$ hours since the GRB onset, with the 0.11 m telephoto lenses of the Livermore Optical Transient Imaging System (0.11LOTIS), in California (USA). 0.11LOTIS uses a 2×2 CCD array. Each CCD is a 2048×2048 Loral 442A, giving a $8.8^\circ \times 8.8^\circ$ individual field of view (FOV). Collectively the four CCDs provide a $17.4^\circ \times 17.4^\circ$ FOV.

Finland, Iceland, Norway, and Sweden, in Spain's Observatorio del Roque de los Muchachos, of the Instituto de Astrofísica de Canarias.

[†] Based in part on observations made at the European Southern Observatory, in La Silla, Chile (ESO Large Programmes 165.H-0464(A), 165.H-0464(G) and 165.H-0464(I)).

[‡] Based in part on observations made with the Livermore Optical Transient Imaging System's 0.11 m telephoto lenses, at the Lawrence Livermore National Laboratory, in California, USA.

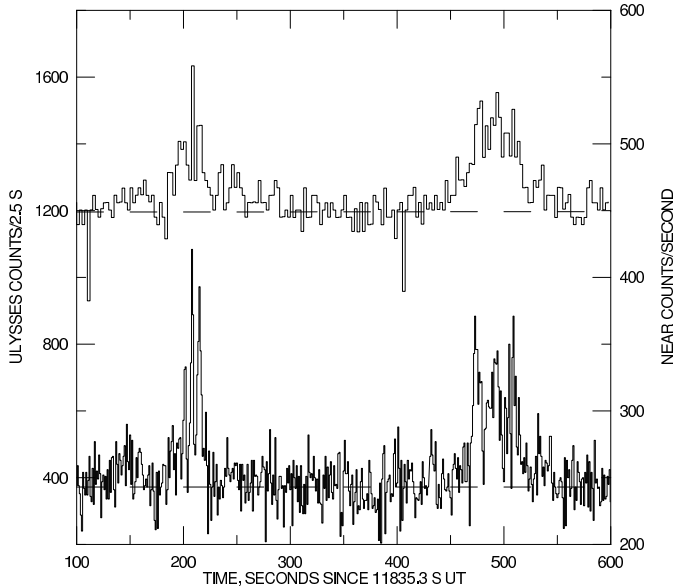


Fig. 1. Ulysses (upper plot) and NEAR (lower plot) time histories for the GRB 001007. The Ulysses data have been taken in the 25–150 keV band, and the NEAR data have been taken in the range >150 keV. Dashed lines indicate the backgrounds.

Target of Opportunity programmes were triggered starting at $t_0 + 93.26$ hours at, the 0.82 m telescope of the Instituto de Astrofísica de Canarias (0.82IAC) at the Observatorio del Teide, in the island of Tenerife (Spain), the 1.54 m Danish telescope (1.54D) at the European Southern Observatory, in La Silla (Chile) and the 2.56 m Nordic Optical Telescope (2.56NOT) at the Observatorio del Roque de los Muchachos, in the island of La Palma (Spain). The CCD used at the 0.82IAC is a 1024×1024 Thomson, giving a $7.3' \times 7.3'$ FOV. The CCD used at the 1.54D (+DFOSC) is a 2048×2048 MAT/EEV, giving a $13.8' \times 13.8'$ FOV. The CCD used at the 2.56NOT (+ALFOSC) is a 2048×2048 Loral/Lesser, giving a $6.5' \times 6.5'$ FOV.

Further deep images were acquired in order to detect the underlying host galaxy with the European Southern Observatory 3.60 m telescope (3.60ESO), in La Silla (Chile). The CCD used at the 3.60ESO (+EFOSC2) is a 2048×2048 Loral, giving a $5.4' \times 5.4'$ FOV. Recently deep R-band images have been obtained at the 8.2-m UT3 of the Very Large Telescope (8.2VLT), 468 days after the burst. The 8.2VLT observations were carried out with FORS1, which based on a 2048×2048 TK2048EB4-1 CCD provides a $6.8' \times 6.8'$ FOV. Table 1 displays the observing log.

We performed aperture photometry using the PHOT routine under IRAF¹. The field was calibrated observing the Landolt fields Rubin 149 and T Phe (Landolt 1992) at airmasses similar to that of the GRB field. Table 2 shows the position and magnitude of three secondary standards close to the OA position (see Fig. 2).

¹ IRAF is distributed by the National Optical Astronomy Observatories, which are operated by the Association of Universities for Research in Astronomy, Inc., under cooperative agreement with the US National Science Foundation.

Table 1. Journal of observations of the GRB 001007 field.

| Date UT | Telescope | Filtre | Seeing (arcseconds) | Exposure Time (seconds) | Magnitude |
|-------------------------|------------------|----------|------------------------|----------------------------|--------------|
| 07.4632–07.4645/10/2000 | 0.11LOTIS(CCD) | <i>V</i> | § | 2 × 50 | > 15.52 * |
| 08.4630–08.4643/10/2000 | 0.11LOTIS(CCD) | <i>V</i> | § | 2 × 50 | > 15.52 * |
| 11.0932–11.2222/10/2000 | 0.82IAC (CCD) | <i>R</i> | 2.50 | 4 × 1800 | 20.50 ± 0.13 |
| 11.1151–11.2008/10/2000 | 0.82IAC (CCD) | <i>B</i> | 2.65 | 2 × 1800 | 21.39 ± 0.20 |
| 11.2232–11.2440/10/2000 | 0.82IAC (CCD) | <i>V</i> | 2.75 | 1800 | 20.96 ± 0.25 |
| 11.3192–11.3673/10/2000 | 1.54D (DFOSC) | <i>R</i> | 0.95 | 4 × 600 | 20.77 ± 0.06 |
| 12.2517–12.2641/10/2000 | 0.82IAC (CCD) | <i>R</i> | 2.85 | 1069 | > 20.30 ** |
| 20.2366–20.2437/10/2000 | 2.56NOT (ALFOSC) | <i>R</i> | 1.00 | 600 | > 22.10 ** |
| 29.2584–29.3074/10/2000 | 1.54D (DFOSC) | <i>R</i> | 0.85 | 6 × 600 | 23.98 ± 0.17 |
| 02.1368–02.1676/11/2000 | 3.60ESO (EFOSC2) | <i>R</i> | 0.70 | 5 × 500 | 24.00 ± 0.16 |
| 02.1683–02.2049/11/2000 | 3.60ESO (EFOSC2) | <i>B</i> | 0.90 | 5 × 600 | 24.90 ± 0.25 |
| 09.0788–09.0892/11/2000 | 0.82IAC (CCD) | <i>V</i> | 2.25 | 900 | > 21.25 ** |
| 16.1203–16.1718/11/2000 | 3.60ESO (EFOSC2) | <i>R</i> | 0.60 | 7 × 600 | 24.53 ± 0.22 |
| 13.3770–13.4092/09/2001 | 3.60ESO (EFOSC2) | <i>B</i> | 0.85 | 3 × 900 | † |
| 14.2787–14.2999/09/2001 | 3.60ESO (EFOSC2) | <i>B</i> | 0.70 | 2 × 900 | 25.10 ± 0.25 |
| 18.0544–18.0867/01/2002 | 8.2VLT (FORS1) | <i>R</i> | 0.65 | 8 × 300 | 24.84 ± 0.15 |

§ Irrelevant given the pixel scale, 15 arcseconds/pixel.

* 10σ upper limit (3σ upper limits can not be quoted because 0.11LOTIS under samples the point spread function due to its large pixel scale. The 3σ limit would not be much different than a single pixel noise variation).

** 3σ upper limit.

† The images from 13–14/09/2001 were coadded because of the faintness of the host galaxy, resulting in just a single magnitude, $B = 25.10 \pm 0.25$.

Table 2. Secondary standards in the field of the GRB 001007.

| | RA(J2000) h m s | Dec(J2000) ° ' " | <i>B</i> | <i>V</i> | <i>R</i> |
|---|--------------------|---------------------|--------------|--------------|--------------|
| 1 | 04 06 09.26 | −21 55 23.9 | 19.49 ± 0.07 | 18.30 ± 0.05 | 17.19 ± 0.02 |
| 2 | 04 06 07.94 | −21 55 16.6 | 20.02 ± 0.07 | 18.88 ± 0.08 | 18.05 ± 0.03 |
| 3 | 04 06 04.98 | −21 54 22.5 | 19.79 ± 0.07 | 18.49 ± 0.05 | 17.44 ± 0.03 |

3. Results and discussion

A bright OA was detected in the first 0.82IAC images at the preliminary position given by Price et al. (2000a). An astrometric solution based on 50 USNO A2-0 reference stars in the 1.54D image taken on 11.3192–11.3673 UT October 2000 yields for the OA $\alpha_{2000} = 4^{\text{h}}5^{\text{m}}54.28^{\text{s}}$, $\delta_{2000} = -21^{\circ}53'45.4''$. The internal error of the position is $0.55''$, which has to be added to the 1σ systematic error of the USNO catalogue ($\simeq 0.25''$ according to Assafin et al. 2001). The final astrometric error corresponds to $0.60''$. The upper limits and optical magnitudes of the afterglow are displayed in the far right column of Table 1.

3.1. The spectral shape of the OA: determination of the electron distribution power law index

We have determined the flux distribution of the GRB 001007 OA on 11.15 UT October 2000 (mean epoch of the first *B* band image) by means of our *BVR* broad band photometric measurements obtained with the 0.82IAC. We fitted the ob-

served flux distribution with a power law $F_{\nu} \propto \nu^{\beta}$, where F_{ν} is the flux at frequency ν , and β is the spectral index. The optical flux at the wavelengths of *B*, *V* and *R* bands have been derived by subtracting the contribution of the host galaxy (see Sect. 3.4), assuming a reddening $E(B - V) = 0.042$ from the DIRBE/IRAS dust maps (Schlegel et al. 1998) and, correcting for the epoch differences (assuming $\alpha = -2.05 \pm 0.11$, calculated in Sect. 3.2). In converting the magnitude into flux, the effective wavelengths and normalisations given in Fukugita et al. (1995) were used (assuming for α Lyr, $V = 0.03$, $B - V = 0$, $V - R_c = 0$). The flux densities are 13.0, 17.5, and $21.3 \mu\text{Jy}$ at the *B*, *V* and *R* bands, corrected by Galactic reddening (but not for possible intrinsic absorption in the host galaxy). The fit to the optical data $F_{\nu} \propto \nu^{\beta}$ gives $\beta = -1.24 \pm 0.57$.

In the expression of the spectral index ($F_{\nu} \propto \nu^{\beta}$) β only depends on p and is independent of the geometry of the expansion. For an adiabatic expansion it is given by $\beta = (1 - p)/2$ for $\nu_c > \nu > \nu_m$ and by $\beta = -p/2$ for $\nu > \nu_c$, where ν is the observing frequency and ν_c is the cooling break frequency (Sari et al. 1998).

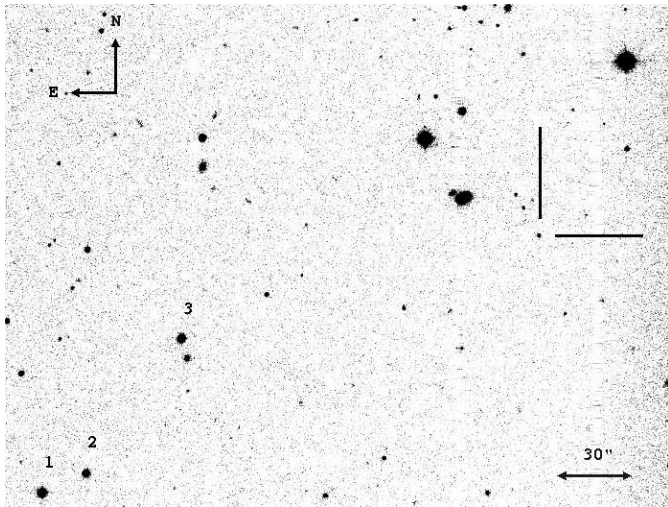


Fig. 2. R band image of the GRB 001007 field taken at the 1.54D on 11.3192–11.3673 October 2000. The position of the OA is indicated between tick marks. The numbered stars represent secondary standards logged in Table 2. North is upwards and East leftwards.

The values we have derived for p are 3.48 ± 1.14 ($\nu_c > \nu > \nu_m$), and 2.48 ± 1.14 ($\nu > \nu_c$). The value of p for the afterglows detected to date range from 2 to 2.5 (van Paradijs et al. 2000). Thus, given the advanced stage of the afterglow evolution (~ 4 days after the GRB) at which our spectral energy distribution (SED) was constructed and, the values of p derived above, we consider that our BVR band frequencies are much more consistent with the $\nu > \nu_c$ regime.

3.2. The lightcurve of the GRB 000107 OA

Our B and R band lightcurves (Fig. 3) show that the source was declining in brightness. The optical decay slowed down in early November 2000 suggesting the presence of an underlying source of constant brightness: the host galaxy. The deep 8.2VLT images taken in January 2002 confirmed this fact.

Most GRB optical counterparts appear to be well characterised by a power law decay plus a constant flux component, $F(t) \propto (t - t_0)^\alpha + F_{\text{host}}$ where, $F(t)$ is the total measured flux of the counterpart at time $(t - t_0)$ after the onset of the event at t_0 , α is the temporal decay index and F_{host} is the flux of the underlying host galaxy. F_{host} can be fixed or considered as a free parameter.

In order to test the self-consistency of our R band data, we considered all the R band points except that late VLT observation leaving F_{host} as a free parameter. By means of fitting least square linear regression to the observed R band fluxes, we predict for the host galaxy $R = 24.79 \pm 0.22$. This value is fully consistent with the R band magnitude measured with the VLT ($R = 24.84 \pm 0.15$), supporting the VLT identification as the host galaxy. Fixing the R band host galaxy magnitude to $R = 24.84 \pm 0.15$, a power law decline with $\alpha_R = -2.05 \pm 0.11$ ($\chi^2/\text{dof} = 0.54$) provides a good fit to the R band data (see lower panel of Fig. 3).

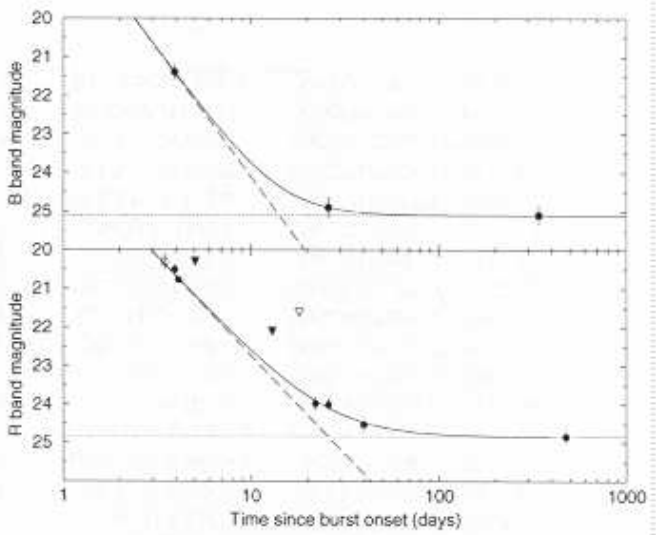


Fig. 3. B and R band lightcurves of the OA related to the GRB 001007, including the underlying galaxy. Circles represent measured magnitudes and triangles represent upper limits. Filled symbols are our data points whereas empty ones are data points from the literature, the circle is from Price et al. (2000a) and the triangle from Price et al. (2000b). The dashed and dotted lines show the two components of our fit, the OA component (with $\alpha_B = -2.65 \pm 0.73$ and $\alpha_R = -2.05 \pm 0.11$) and the host galaxy component (with $B = 25.10$ and $R = 24.84$). The sum of both components yields the solid line.

This value is also consistent with the B band observations, which can be fitted by a power law decline with $\alpha_B = -2.65 \pm 0.73$ (the host magnitude has been fixed at $B = 25.10 \pm 0.25$; based on our late epoch imaging, see Sect. 3.4). Thus, our data can be explained by an achromatic decay. Assuming $\alpha = \alpha_R = -2.05 \pm 0.11$, the flux decay of the GRB 001007 is one of the steepest declines for all GRBs observed so far.

In order to see if a break exists in the light curve we have made use of the constraints derived from the early data taken with 0.11LOTIS. We have extrapolated the R band lightcurve to the epoch of the first 0.11LOTIS observations (7.4638 UT October 2000). The prediction yields $R = 14.56 \pm 0.34$. This value has been dereddened from Galactic extinction (Schlegel et al. 1998) and then extrapolated to the V band, making use of the derived value of β (see Sect. 3.1). Finally, this value is reddened back in order to make it comparable to the 0.11LOTIS V band upper limit measurement. This procedure yielded $V = 15.02 \pm 0.36$. This value is 1.4σ above the upper limit imposed by 0.11LOTIS (see Table 1). Therefore, the 0.11LOTIS upper limit suggests the existence of a break in the lightcurve.

If the contribution of an underlying supernova were to be present in the lightcurve then, it is expected to peak at $\sim 15(1+z)$ days. The GRB 001007 is a good candidate for such a search thanks to its rapid decay but, the sparse R band coverage makes this search elusive.

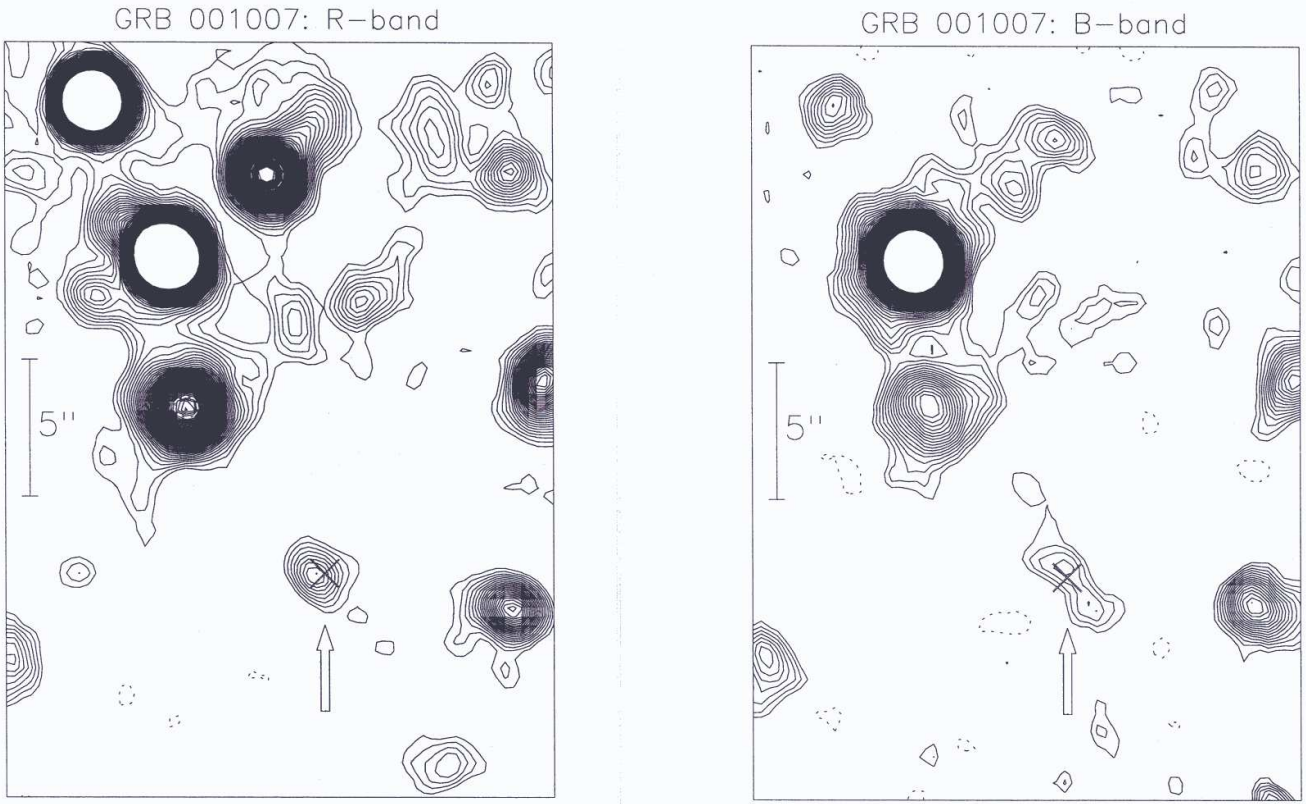


Fig. 4. Contour plot displaying the host galaxy of the GRB 001007 and the position of its OA. **Left panel:** it shows the coadded *R* band image taken from 16.1203 UT to 16.1718 UT November 2000 at the 3.60ESO telescope, with still significant contribution from the OA. **Right panel:** it shows the coadded *B* band image taken from 13.3770 UT to 13.4092 UT, and from 14.2787 UT to 14.2999 UT, September 2001 at the 3.60ESO telescope, with negligible contribution from the OA. **General:** Both sets of images revealed the presence of an extended and elongated object in the Northeast-Southwest direction ($PA \sim +45^\circ$). The position of the OA is indicated by a cross and, in both filters, it is fully consistent with it. The *B*-band image suggested that the source was part of a complex object. Further VLT images confirmed (see Fig. 5) that this extended source is in fact composed by at least two objects. The complexity of the object can not be visualized in the *R*-band image displayed in the right panel, likely by the non negligible contribution of the afterglow on 16.1203–16.1718 UT November 2000. The position of the cross was calculated by transforming the image taken with the 1.54D (11.3192 UT–11.3673 UT October 2000, where the OA is clearly visible) to the frames of the 3.60ESO coadded images which are listed above. The error of the cross position (including frame alignment errors and internal astrometric errors) is $\sim 0.7''$, smaller than its size ($1'' \times 1''$). See Fig. 5 for a more accurate view of the OA position. North is upwards and East leftwards.

3.3. Comparison of the lightcurve with predictions made by several models

Many OAs exhibit a single power law decay index. Generally this index is $\alpha \sim -1.3$, a reasonable value for the spherical expansion of a relativistic blast wave in a constant density interstellar medium (Mészáros & Rees 1997). Nonetheless there are OAs for which a break occurs within 2 days of the burst. This break has been seen and modelled as a signature of beaming. We note that collimated outflows in general result in faster decaying lightcurves than the spherically symmetric ones (Huang et al 2000).

We quantify a break as $\Delta\alpha = \alpha_1 - \alpha_2$, where α_1 is the decay index before the break and α_2 after the break. Six afterglow models have been considered in order to reproduce our values of α and β :

i) An outflow arising in a jet expanding sideways in a homogeneous medium; then $\alpha_1 = 3(1-p)/4$ and $\alpha_2 = -p$ (Rhoads 1999). In this case, $p = 2.05 \pm 0.11$, and we would expect $\alpha_1 = 0.79 \pm 0.08$, and $\beta = -1.03 \pm 0.06$, what agrees fully with our data. This case would resemble GRB 990510, for which $\alpha_1 = -0.82 \pm 0.02$, $\alpha_2 = -2.18 \pm 0.05$ and a break occurred at $t_0 = 1.20 \pm 0.08$ days after the GRB (Harrison et al. 1999).

ii) A collimated outflow with a fixed opening angle in a homogeneous medium; then $\Delta\alpha = 0.75$ (Mészáros & Rees 1999). Here $\alpha_1 = 3(1-p)/4$ changes to $\alpha_2 = -3p/4$ in the optical range, considering an adiabatic outflow (Panaitescu & Mészáros 1999). Following this model $p = 2.73 \pm 0.15$, $\alpha_1 = -1.30 \pm 0.11$, and $\beta = -1.37 \pm 0.08$, in agreement with the measured spectral index.

iii) A collimated outflow with a fixed opening angle in an inhomogeneous medium (density gradient $\rho \propto r^{-s}$, with $s = 2$ as expected in a stellar wind, Panaitescu et al. 1998); then $\Delta\alpha = (3 - s)/(4 - s)$, changing from $\alpha_1 = -3(p - 1)/4 - (s/8 - 2s)$ to $\alpha_2 = -3(p - 1)/4 - (6 - s)/(8 - 2s)$. For $s = 0$ we recover ii). In general, if the mean density distribution is not constant the light curve decays faster but, the break will be less pronounced. For the case of our α value, and assuming $s = 2$, we derive $p = 2.40 \pm 0.15$, $\alpha_1 = -1.55 \pm 0.11$, and $\beta = -1.20 \pm 0.08$, also consistent with our value of $\beta = -1.24 \pm 0.57$. This case would be similar to GRB 980519 where the decay index changed from $\alpha_1 = -1.73 \pm 0.04$ to $\alpha_2 = -2.22 \pm 0.04$ at $t_0 = 0.55$ days after the gamma ray event (Jaunsen et al. 2001).

The outcome of α_1 in the three jet models discussed above falls within the boundaries defined by the observations made to date, from -0.76 ± 0.01 in the GRB 990510 (Harrison et al. 1999; Stanek et al. 1999) to -1.73 ± 0.04 in the GRB 980519, Jaunsen et al. 2001.

iv) The late evolution of highly relativistic jets of cannon balls emitted in supernova explosions. This model predicts a smooth knee having an after the break decay index $\alpha_2 = -2.1$, and a spectral index $\beta = -1.1$, fully consistent with our data (Dado et al. 2001).

v) A spherical adiabatic expansion with $\rho \propto r^{-s}$; we have a monotonic power law decay with $\alpha = -3(p - 1)/4 - s/(8 - 2s)$. For $s = 2$ (inhomogeneous medium due to a stellar wind) a value of $p = 3.07 \pm 0.15$ and $\beta = -1.54 \pm 0.08$ is expected. Although the derived value of β is consistent with the measurements, the large value of p is out of the range derived for the afterglows observed so far (p ranges from 2 to 2.5). Thus, we consider this option less reconcilable with the data.

vi) For $s = 0$ (a spherical adiabatic expansion in an homogeneous medium) even more unrealistic values of p are obtained ($p = 3.73$). The derived value of the decay index α can not be easily accommodated in this model. In fact, the fastest decay seen so far for a well sampled monotonic power law decay corresponds to the GRB 990705 with $\alpha = -1.68 \pm 0.10$ (Masetti et al. 2000), inconsistent with our α .

On the light of the previous arguments we propose that the observed steep decay in the optical lightcurve may be due to a break which occurred before the optical observations started, ~ 3.5 days after the burst, and explainable in the context of i), ii), iii) and iv). This conclusion is supported by the knee suggested by the prompt 0.11LOTIS data (see Section 3.2.)

3.4. The potential host galaxy

Inspection of the B band images taken in September 2001 with the 3.60ESO telescope suggested the presence of a faint object coincident with the position of the OA reported in Sect. 3 (see cross of Fig. 4). Further R-band VLT imaging carried out ~ 468 days after the gamma-ray event confirmed these evidences, detecting clearly the object previously imaged with the 3.60ESO. Its non stellar profile (the angular extension of the source is $\sim 5''$) and its consistency with the OA position makes it a strong candidate to be the host galaxy of the GRB 001007.

The excellent (seeing $0.65''$) VLT observations revealed the complex morphology of the host galaxy (see Fig. 5). The host is composed by at least two objects, 6σ and 9σ above the local background level, respectively. The position of these two sources are; $\alpha_{2000} = 4^{\text{h}}5^{\text{m}}54.19^{\text{s}}$, $\delta_{2000} = -21^{\circ}53'46.7''$ and $\alpha_{2000} = 4^{\text{h}}5^{\text{m}}54.34^{\text{s}}$, $\delta_{2000} = -21^{\circ}53'44.6''$ (error $0.6''$ in both cases). Between these two sources there is a faint source (only 3σ above the background level) located at $\alpha_{2000} = 4^{\text{h}}5^{\text{m}}54.28^{\text{s}}$, $\delta_{2000} = -21^{\circ}53'45.3''$. Only this third possible component is consistent with the 1σ astrometric circle (see Fig. 5). The two brightest components are located between 2σ and 3σ from the OA position, so their possible connection with the OA can not be discarded.

Circular aperture photometry (aperture diametre $6''$) yielded $B = 25.10 \pm 0.25$ and $R = 24.84 \pm 0.15$ for the host galaxy complex. The underreddened (by Galactic extinction) fluxes imply a blue spectral distribution ($F_{\nu} \propto \nu^{\beta}$, with $\beta \sim 0.26$) as expected in the UV rest frame for a star forming galaxy. In fact, comparison between the VLT R-band and the 3.60ESO B-band images reveals that the closest system (the one to the North-East from the OA, see Fig. 5) to the OA position is the bluest one. From the fit we interpolate at the frequency corresponding to the V band ($\nu_V = 5.45 \times 10^{14}$ Hz) and derive a V band flux of $0.42 \mu\text{Jy}$. The inferred V -band flux as well as the measured BR band fluxes ($0.44 \mu\text{Jy}$ and $0.40 \mu\text{Jy}$, both corrected by Galactic extinction) were used in Sect. 3.1 to subtract the contribution of the host to the total measured flux.

4. Conclusions

We presented observations of the OA associated with the GRB 001007 and its likely host galaxy, starting 6.14 hours after the event and continuing up to $t_0 + \sim 468$ days. The R band lightcurve is well fitted by a power law plus a constant brightness component due to the host galaxy. The decay indices in the B and R bands are $\alpha_R = -2.05 \pm 0.11$ and $\alpha_B = -2.65 \pm 0.73$. They are consistent with each other suggesting that the decay is achromatic, so we assumed $\alpha = \alpha_R$ throughout the paper. The BVR band observations carried out at ~ 11.15 UT October 2000 allowed us to determine a spectral index $\beta = -1.24 \pm 0.57$.

Several models were considered to explain our value of α and β . The existence of a jet is supported but we can not distinguish between the different jet geometries and density profiles of the GRB environment. An alternative explanation can be provided by the late evolution of highly relativistic jets of cannon balls emitted in supernova explosions. A spherical expansion in an inhomogeneous medium is marginally consistent with our data (because of poor sampling of the lightcurve and the SED). A spherical expansion in a homogeneous medium is inconsistent.

We proposed that the observed steep decay in the optical lightcurve may be due to a break which occurred before the OA was discovered, ~ 3.5 days after the burst. A relativistic jet expansion (fireball or cannonball) could explain the fast decay as well as the proposed break. This suggestion is supported by the upper limits derived from our prompt optical observations. The extrapolation of the R-band lightcurve to epoch of the ob-

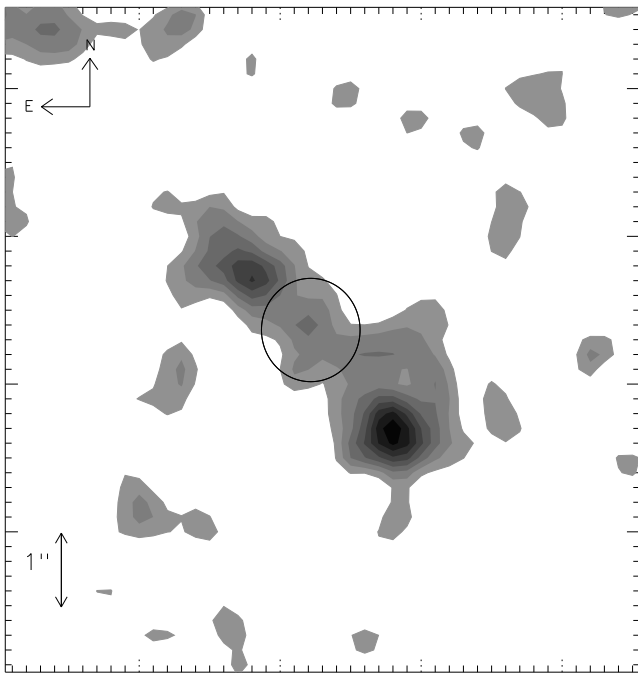


Fig. 5. The figure shows the GRB 001007 field imaged with the VLT ~ 468 days after the gamma-ray event. The image corresponds to an integration time of 2400 s in the R-band. The circle indicates the position of the afterglow. Its radius corresponds to the astrometric and alignment errors (0.7''). As in Fig. 4 the afterglow position has been derived using the image taken with the 1.54D (11.3192 UT–11.3673 UT October 2000) and transforming it to the VLT image frame. The image has been smoothed with a Gaussian filter with a FWHM of 1 pixel (0.2''). As can be seen an extended object is consistent with the afterglow position. The contours scale linearly starting from 1σ above the background. This smoothed image shows that the object is composed by at least two sources, 6σ and 9σ above the local background level, respectively. A possible third component (3σ above the background) can be seen inside the astrometric circle.

servations carried out by 0.11LOTIS, predicts $R=14.56 \pm 0.34$ and $V = 15.02 \pm 0.36$. These values are 1.4σ above the upper limit imposed by 0.11LOTIS, therefore suggesting the presence of a knee in the optical light curve.

The potential host galaxy is in a complex system with integrated magnitudes $B = 25.10 \pm 0.25$ and $R = 24.84 \pm 0.15$. Its overall spectral distribution is consistent with a rest frame star forming galaxy. The system shows a complex morphology, being composed by at least two components, with the bluest one being closer to the OA. Deep observations with the Hubble Space Telescope are required to study the nature of the system and the precise location of the OA within it, determining whether the knot seen at a 3σ level at the OA position would be a star-forming region associated to the bluest component or not.

Acknowledgements. J.M. Castro Cerón acknowledges the receipt of a FPI doctoral fellowship from Spain's Ministerio de Ciencia y Tecnología and the hospitality of the Danish Space Research Institute and the Instituto de Astrofísica de Andalucía (CSIC) where part of

this work was carried out. J. Gorosabel acknowledges the receipt of a Marie Curie Research Grant from the European Commission. This work was partially supported by Denmark's Natural Science Research Council through its Centre for Ground Based Observational Astronomy. The data presented here have been taken in part using ALFOSC, which is owned by the Instituto de Astrofísica de Andalucía (IAA) and operated at the Nordic Optical Telescope under agreement between IAA and the NBIfAFG of the Astronomical Observatory of Copenhagen. Some of the observations presented in this paper were obtained under the ESO Large Programme 165.H-0464.

References

Andersen, M.I., Hjorth, J., Pedersen, H., et al. 2000, A&A, 364, L54.
 Assafin, M., Andrei, A.H., Vieira Martins, R., et al. 2001, ApJ, 552, 380.
 Castro-Tirado, A.J., Grosdidier, Y., Castro Cerón, J.M., et al. 2000, GCN, 845.
 Dado, S., Dar, A., & De Rújula, A. 2001, A&A, submitted [astro-ph/0107367].
 Frail, D., & Berger, E. 2000, GCN, 860.
 Fishman, G.J., & Meegan, C.A. 1995, ARA&A, 33, 415.
 Fukugita, M., Shimasaku, K., & Ichikawa, T. 1995, PASP, 107, 945.
 Galama, T.J., Vreeswijk, P.M., van Paradijs, J. et al., 1998, Nature, 395, 670.
 Harrison, F.A., Bloom, J.S., Frail, D.A., et al. 1999, ApJ, 523, L121.
 Axelrod
 Huang, Y.F., Dai, Z.G. & Lu, T. 2000, A&A, 355, L43.
 Hurley, K., Cline, T., Mazets, E., & Golenetskii, S. 2000, GCN, 841.
 Jaunsen, A.O., Hjorth, J., Björnsson, G., et al. 2001, ApJ, 546, 127.
 Landolt, A.U. 1992, AJ, 104, 340.
 Masetti, N., Palazzi, E., Pian, E., et al. 2000, A&A, 354, 473.
 Mészáros, P., & Rees, M.J. 1997, ApJ, 476, 232.
 Mészáros, P., Rees, M.J., & Wijers, R.A.M.J. 1998, ApJ, 499, 301.
 Mészáros, P., & Rees, M.J. 1999, MNRAS, 306, L39.
 Panaiteescu, A., Mészároz, P., & Rees, M.J. 1998, ApJ, 503, 314.
 Panaiteescu, A., & Mészároz, P., 1999, ApJ, 526, 707.
 Price, P.A., Aselrod, T.S., & Schmidt, B.P. 2000a, GCN, 843.
 Price, P.A., Penunova, O., Madore, B., & Djorgovski, S.G. 2000b, GCN, 862.
 Rhoads, J.E. 1999, ApJ, 525, 737.
 Sari, R., Piran, T., & Narayan, R. 1998, ApJ, 497, L17.
 Schlegel, D.J., Finkbeiner, D.P., & Davis, M. 1998, ApJ, 500, 525.
 Stanek, K.Z., Garnavich, P.M., Kaluzny, J., Pych, W., & Thompson, I. 1999, ApJ, 522, L39.
 van Paradijs, J., Kouveliotou, C., & Wijers, R.A.M.J. 2000, ARA&A, 38, 379.